Flexural-torsional behavior of thin-walled composite box beams using shear-deformable beam theory

Thuc Phuong Vo* and Jaehong Lee†

Department of Architectural Engineering, Sejong University
98 Kunja Dong, Kwangjin Ku, Seoul 143-747, Korea

(Dated: June 4, 2007)

This paper presents a flexural-torsional analysis of composite box beams. A general analytical model applicable to thin-walled composite box beams subjected to vertical and torsional load is developed. This model is based on the shear-deformable beam theory, and accounts for the flexural response of the thin-walled composites for arbitrary laminate stacking sequence configuration, i.e. unsymmetric as well as symmetric. Governing equations are derived from the principle of the stationary value of total potential energy. Numerical results are obtained for thin-walled composites under vertical loading, addressing the effects of fiber angle and span-to-height ratio of the composite beam.

Keywords: thin-walled composites, shear deformation, flexural-torsional response, finite element method

I. INTRODUCTION

Fiber-reinforced composite materials have been used over the past few decades in a variety of structures. Composites have many desirable characteristics, such as high ratio of stiffness and strength to weight, corrosion resistance and magnetic transparency. Thin-walled structural shapes made up of composite materials, which are usually produced by pultrusion, are being increasingly used in many engineering fields. In particular, the use of pultruded composites in civil engineering structures await increased attention.

Thin-walled composite structures are often very thin and have complicated material anisotropy. Accordingly, warping and other secondary coupling effects should be considered in the analysis of thin-walled composite structures. The theory of thin-walled closed section members made of isotropic materials was first developed by Vlasov [1] and Gjelsvik [2]. For fiber-reinforced composites, some analyses have been formulated to analyze composite box beams with varying levels of assumptions. Chandra et al. [3] discussed the structural couplings effects for symmetric and anti-symmetric box beams under flexural, torsional, and extensional loads. Smith and Chopra [4] formulated and evaluation of an analytical model for composite box-beams. The box-beams walls were modeled as orthotropic-ply laminated plates, so that the elastic properties vary both through the thickness and around the box-beams contour; deformation is described in terms of extension, bending, twisting, shearing, and torsion-related out- of-plane warping. Song and Librescu [5] focused on the formulation of the dynamic problem of laminated composite thick- and thin-walled, single-cell beams of arbitrary cross-section and on the investigation of their associated free vibration behavior. Qin and Librescu [6] provided further contribution and validations on a shear-deformable theory of anisotropic thin-walled beams. The solution methodology was based on the Extended Galerkin's Method and the non-classical effects on the static responses and natural frequencies were investigated. Kim and White [7,8] developed an efficient method to account for 3-dimensional elastic effects in laminated beam walls. In this analysis primary and secondary torsional warping and transverse shear effects, both of the cross-section and of the beam walls, were considered. Pluzsik and Kollar [9] presented a beam theory for thin-walled open and closed section composite beams which analyzes the effect of shear deformation and restrained warping. Salim and Davalos [10] presented the linear analysis of open and closed sections made of general laminated composites by extending Gjelsvik's model [2]. This model accounted for all possible elastic couplings in composite sections, such as extension- and bending-torsion. The effect of warping-torsion on the torsional stiffness of the beam was investigated. Recently, Librescu and Song [11] introduced the monograph about thin-walled composite beams. The monograph was concerned not only with the foundation and formulation of

*Graduate student

†Associate Professor, corresponding author
; Electronic address: jhlee@sejong.ac.kr

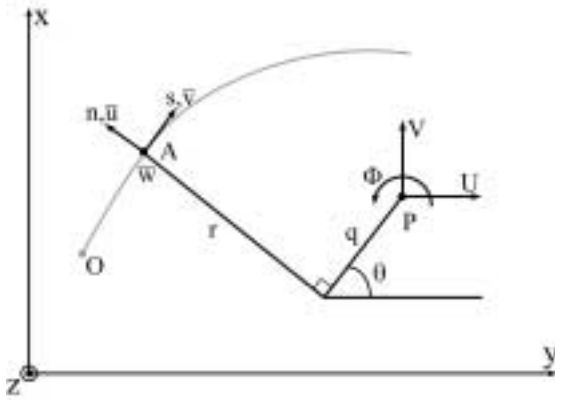

FIG. 1 Definition of coordinates and generalized displacements in thin-walled closed sections

modern linear and nonlinear theories of composite thin-walled beams but also provided powerful mathematical tools to address issues of statics and dynamics of composite thin-walled beam. The effects of transverse shear, warping inhibition, and of various elastic couplings on the behavior of these structures, have been highlighted. Piovan and Cortinez [12] presented a new theoretical model for the generalized linear analysis of thin-walled beams with open or closed cross-sections. The model was developed by employing a non-linear displacement field and allowed studying many problems of static, free vibrations with or without arbitrary initial stresses and linear stability of composite thin-walled beams with general cross-sections. More recently, Vo and Lee [13] presented analytical model which accounts for flexural-torsional behavior of composite box beams. They developed one-dimensional finite element model to investigate the flexural-torsional behavior of thin-walled composite beams.

In this paper, an analytical model for thin-walled open-section composite beams developed by Lee [14] has been extended to the composite box beams. This model is based on the first-order shear deformable beam theory, and accounts for all the structural coupling coming from the material anisotropy. Governing equations are derived from the principle of the stationary value of total potential energy. Numerical results are obtained for thin-walled composites under vertical loading, addressing the effects of fiber angle and span-to-height ratio of the composite beams.

II. KINEMATICS

The theoretical developments presented in this paper require two sets of coordinate systems which are mutually interrelated. The first coordinate system is the orthogonal Cartesian coordinate system (x, y, z), for which the x and y axes lie in the plane of the cross section and the z axis parallel to the longitudinal axis of the beam. The second coordinate system is the local plate coordinate (n, s, z) as shown in Fig.1, wherein the n axis is normal to the middle surface of a plate element, the s axis is tangent to the middle surface and is directed along the contour line of the cross section. The (n, s, z) and (x, y, z) coordinate systems are related through an angle of orientation θ as defined in Fig.1. Point P is called the pole axis, through which the axis parallel to the z axis is called the pole axis.

To derive the analytical model for a thin-walled composite beam, the following assumptions are made

1. The contour of the thin wall does not deform in its own plane.

2. Transverse shear strains $\gamma^{\circ}_{xz}, \gamma^{\circ}_{yz}$ and warping shear γ°_{ω} are incorporated. It is assumed that they are uniform over the cross-sections.

3. The linear shear strain $\bar{\gamma}_{sz}$ of the middle surface is to have the same distribution in the contour direction as it does in the St. Venant torsion in each element.

According to assumption 1, the midsurface displacement components $\bar{u}, \bar{v}$ at a point A in the contour coordinate system can be expressed in terms of a displacements U, V of the pole P in the x, y directions, respectively, and the rotation angle Φ about the pole axis

$$\bar{u}(s,z) = U(z)\sin\theta(s) - V(z)\cos\theta(s) - \Phi(z)q(s) \tag{1a}$$

$$\bar{v}(s,z) = U(z)\cos\theta(s) + V(z)\sin\theta(s) + \Phi(z)r(s) \tag{1b}$$

These equations apply to the whole contour. The out-of-plane shell displacement $\bar{w}$ can now be found from the assumption 2. For each element of middle surface, the midsurface shear strains in the contour can be expressed with respect to the transverse shear and the warping shear strains

$$\bar{\gamma}_{nz}(s,z) = \gamma^{\circ}_{xz}(z)\sin\theta(s) - \gamma^{\circ}_{yz}(z)\cos\theta(s) + \gamma^{\circ}_{\omega}(z)q(s) \tag{2a}$$

$$\bar{\gamma}_{sz}(s,z) = \gamma^{\circ}_{xz}(z)\cos\theta(s) + \gamma^{\circ}_{yz}(z)\sin\theta(s) - \gamma^{\circ}_{\omega}(z)r(s) - \Big[\gamma^{\circ}_{\omega}(z) - \Phi'(z)\Big]\frac{F(s)}{t(s)} \tag{2b}$$

where $t(s)$ is the thickness of contour box section, $F(s)$ is the St. Venant circuit shear flow. Further, it is assumed that midsurface shear strain in $s-n$ direction is zero ($\bar{\gamma}_{sn}=0$). From the definition of the shear strain, $\bar{\gamma}_{sz}$ can also be given for each element of middle surface as

$$\bar{\gamma}_{sz}(s,z) = \frac{\partial \bar{v}}{\partial z} + \frac{\partial \bar{w}}{\partial s} \tag{3}$$

After substituting for $\bar{v}$ from Eq.(1) into Eq.(3) and considering the following geometric relations

$$dx = ds\cos\theta \tag{4a}$$

$$dy = ds\sin\theta \tag{4b}$$

Displacement $\bar{w}$ can be integrated with respect to s from the origin to an arbitrary point on the contour

$$\bar{w}(s,z) = W(z) + \Psi_y(z)x(s) + \Psi_x(z)y(s) + \Psi_\omega(z)\omega(s) \tag{5}$$

where Ψ_x, Ψ_y and Ψ_ω represent rotations of the cross section with respect to x, y and ω, respectively, given by

$$\Psi_y = \gamma^{\circ}_{xz}(z) - U' \tag{6a}$$

$$\Psi_x = \gamma^{\circ}_{yz}(z) - V' \tag{6b}$$

$$\Psi_\omega = \gamma^{\circ}_{\omega}(z) - \Phi' \tag{6c}$$

When the transverse shear effect is ignored, Eq.(6) degenerate to $\Psi_y = -U'$, $\Psi_x = -V'$ and $\Psi_\omega = -\Phi'$, and as a result, the number of unknown variables reduces to four leading to the Euler-Bernoulli beam model. The prime ($'$) is used to indicate differentiation with respect to z; and ω is the so-called sectorial coordinate or warping function given by

$$\omega(s) = \int_{s_\circ}^{s}\Big[r(s) - \frac{F(s)}{t(s)}\Big]ds \tag{7a}$$

$$\oint_i \frac{F(s)}{t(s)}ds = 2A_i \quad i = 1, ..., n \tag{7b}$$

where $r(s)$ is height of a triangle with the base ds; A_i is the area circumscribed by the contour of the i circuit. The explicit forms of $\omega(s)$, $F(s)$ for box section are given in the Appendix of Ref.[13].

The displacement components u, v, w representing the deformation of any generic point on the profile section are given with respect to the midsurface displacements $\bar{u}, \bar{v}, \bar{w}$ by assuming the first order variation of inplane displacements v, w through the thickness of the contour as

$$u(s,z,n) = \bar{u}(s,z) \tag{8a}$$

$$v(s,z,n) = \bar{v}(s,z) + n\bar{\psi}_s(s,z) \tag{8b}$$

$$w(s,z,n) = \bar{w}(s,z) + n\bar{\psi}_z(s,z) \tag{8c}$$

where, $\bar{\psi}_s$ and $\bar{\psi}_z$ denote the rotations of a transverse normal about the z and s axis, respectively. These functions can be determined by considering that the midsurface shear strains γ_{nz} is given by definition

$$\bar{\gamma}_{nz}(s,z) = \frac{\partial \bar{w}}{\partial n} + \frac{\partial \bar{u}}{\partial z} \tag{9}$$

By comparing Eq.(2) and (9), the function can $\bar{\psi}_z$ can be written as

$$\bar{\psi}_z = \Psi_y\sin\theta - \Psi_x\cos\theta - \Psi_\omega q \tag{10}$$

Similarly, using the assumption that the shear strain γ_{sn} should vanish at midsurface, the function $\bar{\psi}_s$ can be obtained

$$\bar{\psi}_s = -\frac{\partial \bar{u}}{\partial s} \tag{11}$$

The strains associated with the small-displacement theory of elasticity are given by

$$\begin{aligned}
\epsilon_s(s,z,n) &= \bar{\epsilon}_s(s,z) + n\bar{\kappa}_s(s,z) && (12a)\\
\epsilon_z(s,z,n) &= \bar{\epsilon}_z(s,z) + n\bar{\kappa}_z(s,z) && (12b)\\
\gamma_{sz}(s,z,n) &= \bar{\gamma}_{sz}(s,z) + n\bar{\kappa}_{sz}(s,z) && (12c)\\
\gamma_{nz}(s,z,n) &= \bar{\gamma}_{nz}(s,z) + n\bar{\kappa}_{nz}(s,z) && (12d)
\end{aligned}$$

where

$$\begin{aligned}
\bar{\epsilon}_s &= \frac{\partial \bar{v}}{\partial s}; \quad \bar{\epsilon}_z = \frac{\partial \bar{w}}{\partial z} && (13a)\\
\bar{\kappa}_s &= \frac{\partial \bar{\psi}_s}{\partial s}; \quad \bar{\kappa}_z = \frac{\partial \bar{\psi}_z}{\partial z} && (13b)\\
\bar{\kappa}_{sz} &= \frac{\partial \bar{\psi}_z}{\partial s} + \frac{\partial \bar{\psi}_s}{\partial z}; \quad \bar{\kappa}_{nz} = 0 && (13c)
\end{aligned}$$

All the other strains are identically zero. In Eq.(13), $\bar{\epsilon}_s$ and $\bar{\kappa}_s$ are assumed to be zero, and $\bar{\epsilon}_z$, $\bar{\kappa}_z$ and $\bar{\kappa}_{sz}$ are midsurface axial strain and biaxial curvature of the shell, respectively. The above shell strains can be converted to beam strain components by substituting Eqs.(1), (5) and (8) into Eq.(13) as

$$\begin{aligned}
\bar{\epsilon}_z &= \epsilon_z^\circ + x\kappa_y + y\kappa_x + \omega\kappa_\omega && (14a)\\
\bar{\kappa}_z &= \kappa_y \sin\theta - \kappa_x \cos\theta - \kappa_\omega q && (14b)\\
\bar{\kappa}_{sz} &= \kappa_{sz} && (14c)
\end{aligned}$$

where $\epsilon_z^\circ, \kappa_x, \kappa_y, \kappa_\omega$ and κ_{sz} are axial strain, biaxial curvatures in the x and y direction, warping curvature with respect to the shear center, and twisting curvature in the beam, respectively defined as

$$\begin{aligned}
\epsilon_z^\circ &= W' && (15a)\\
\kappa_x &= \Psi_x' && (15b)\\
\kappa_y &= \Psi_y' && (15c)\\
\kappa_\omega &= \Psi_\omega' && (15d)\\
\kappa_{sz} &= \Phi' - \Psi_\omega && (15e)
\end{aligned}$$

The resulting strains can be obtained from Eqs.(12) and (14) as

$$\begin{aligned}
\epsilon_z &= \epsilon_z^\circ + (x + n\sin\theta)\kappa_y + (y - n\cos\theta)\kappa_x + (\omega - nq)\kappa_\omega && (16a)\\
\gamma_{sz} &= \gamma_{xz}^\circ \cos\theta + \gamma_{yz}^\circ \sin\theta + \gamma_\omega^\circ (r - \frac{F}{2t}) + \kappa_{sz}(n + \frac{F}{2t}) && (16b)\\
\gamma_{nz} &= \gamma_{xz}^\circ \sin\theta - \gamma_{yz}^\circ \cos\theta - \gamma_\omega^\circ q && (16c)
\end{aligned}$$

III. VARIATIONAL FORMULATION

Total potential energy of the system is calculated by sum of strain energy and potential energy

$$\Pi = \mathcal{U} + \mathcal{V} \tag{17}$$

where $\mathcal{U}$ is the strain energy

$$\mathcal{U} = \frac{1}{2}\int_v (\sigma_z \epsilon_z + \sigma_{sz}\gamma_{sz} + \sigma_{nz}\gamma_{sz}) dv \tag{18}$$

The strain energy is calculated by substituting Eq.(16) into Eq.(18)

$$\begin{aligned}\mathcal{U} &= \frac{1}{2}\int_v \Big\{\sigma_z\Big[\epsilon_z^\circ + (x+n\sin\theta)\kappa_y + (y-n\cos\theta)\kappa_x + (\omega-nq)\kappa_\omega\Big] \\ &+ \sigma_{sz}\Big[\gamma_{xz}^\circ\cos\theta + \gamma_{yz}^\circ\sin\theta + \gamma_\omega^\circ(r-\frac{F}{2t}) + \kappa_{sz}(n+\frac{F}{2t})\Big] + \sigma_{nz}\Big[\gamma_{xz}^\circ\sin\theta - \gamma_{yz}^\circ\cos\theta - \gamma_\omega^\circ q\Big]\Big\}dv \end{aligned} \tag{19}$$

The variation of the strain energy, Eq.(19), can be stated as

$$\delta\mathcal{U} = \int_0^l (N_z\delta\epsilon_z + M_y\delta\kappa_y + M_x\delta\kappa_x + M_\omega\delta\kappa_\omega + V_x\delta\gamma_{xz}^\circ + V_y\delta\gamma_{yz}^\circ + T\delta\gamma_\omega^\circ + M_t\delta\kappa_{sz})ds \tag{20}$$

where $N_z, M_x, M_y, M_\omega, V_x, V_y, T, M_t$ are axial force, bending moments in the x and y directions, warping moment (bimoment), and tortional moment with respect to the centroid, respectively, defined by integrating over the cross-sectional area A as

$$N_z = \int_A \sigma_z dsdn \tag{21a}$$

$$M_y = \int_A \sigma_z(x+n\sin\theta)dsdn \tag{21b}$$

$$M_x = \int_A \sigma_z(y-n\cos\theta)dsdn \tag{21c}$$

$$M_\omega = \int_A \sigma_z(\omega-nq)dsdn \tag{21d}$$

$$V_x = \int_A (\sigma_{sz}\cos\theta + \sigma_{nz}\sin\theta)dsdn \tag{21e}$$

$$V_y = \int_A (\sigma_{sz}\sin\theta - \sigma_{nz}\cos\theta)dsdn \tag{21f}$$

$$T = \int_A \Big[\sigma_{sz}(r-\frac{F}{2t}) - \sigma_{nz}q\Big]dsdn \tag{21g}$$

$$M_t = \int_A \sigma_{sz}(n+\frac{F}{2t})dsdn \tag{21h}$$

The variation of the work done by the vertical and torsional load can be stated as

$$\delta\mathcal{V} = -\int_0^l (\mathcal{V}_y\delta V + \mathcal{T}\delta\Phi)dz \tag{22}$$

where $\mathcal{V}_y$ is vertical load and $\mathcal{T}$ is applied torsional load. Using the principle that the variation of the total potential energy is zero, the following weak statement is obtained

$$\begin{aligned}0 &= \int_0^l \Big\{N_z\delta W' + M_y\delta\Psi_y' + M_x\delta\Psi_x' + M_\omega\delta\Psi_\omega' + V_x\delta(U'+\Psi_y) + V_y\delta(V'+\Psi_x) \\ &+ T\delta(\Phi'+\Psi_\omega) + M_t\delta(\Phi'-\Psi_\omega) + \mathcal{V}_y\delta V + \mathcal{T}\delta\Phi\Big\}ds \end{aligned} \tag{23}$$

IV. CONSTITUTIVE EQUATIONS

The constitutive equations of a k^{th} orthotropic lamina in the laminate co-ordinate system of box section are given by

$$\begin{Bmatrix}\sigma_z \\ \sigma_{sz}\end{Bmatrix}^k = \begin{bmatrix}\bar{Q}_{11}^* & \bar{Q}_{16}^* \\ \bar{Q}_{16}^* & \bar{Q}_{66}^*\end{bmatrix}^k \begin{Bmatrix}\epsilon_z \\ \gamma_{sz}\end{Bmatrix} \tag{24}$$

where $\bar{Q}_{ij}^*$ are transformed reduced stiffnesses. The transformed reduced stiffnesses can be calculated from the transformed stiffnesses based on the plane stress assumption and plane strain assumption. More detailed explanation can be found in Ref.[16]

The constitutive relation for out-of-plane stress and strain is given by

$$\sigma_{nz} = \bar{Q}_{55}\gamma_{nz} \tag{25}$$

The constitutive equations for bar forces and bar strains are obtained by using Eqs.(16), (21) and (24)

$$\begin{Bmatrix} N_z \\ M_y \\ M_x \\ M_\omega \\ M_t \\ V_x \\ V_y \\ T \end{Bmatrix} = \begin{bmatrix} E_{11} & E_{12} & E_{13} & E_{14} & E_{15} & E_{16} & E_{17} & E_{18} \\ & E_{22} & E_{23} & E_{24} & E_{25} & E_{26} & E_{27} & E_{28} \\ & & E_{33} & E_{34} & E_{35} & E_{36} & E_{37} & E_{38} \\ & & & E_{44} & E_{45} & E_{46} & E_{47} & E_{48} \\ & & & & E_{55} & E_{56} & E_{57} & E_{58} \\ & & & & & E_{66} & E_{67} & E_{68} \\ & & & & & & E_{77} & E_{78} \\ \text{sym.} & & & & & & & E_{88} \end{bmatrix} \begin{Bmatrix} \epsilon_z^\circ \\ \kappa_y \\ \kappa_x \\ \kappa_\omega \\ \kappa_{sz} \\ \gamma_{xz}^\circ \\ \gamma_{yz}^\circ \\ \gamma_\omega^\circ \end{Bmatrix} \tag{26}$$

where E_{ij} are stiffnesses of the thin-walled composite. ($E_{i,5}, E_{i,8} \quad i = 1..8$) can be defined by

$$E_{15} = \int_s (A_{16}\frac{F}{2t} + B_{16})ds \tag{27a}$$

$$E_{18} = \int_s A_{16}(r - \frac{F}{2t})ds \tag{27b}$$

$$E_{25} = \int_s \Big[A_{16}\frac{F}{2t}x + B_{16}(x + \frac{F\sin\theta}{2t}) + D_{16}\sin\theta\Big]ds \tag{27c}$$

$$E_{28} = \int_s (A_{16}x + B_{16}\sin\theta)(r - \frac{F}{2t})ds \tag{27d}$$

$$E_{35} = \int_s \Big[A_{16}\frac{F}{2t}y + B_{16}(y - \frac{F\cos\theta}{2t}) - D_{16}\cos\theta\Big]ds \tag{27e}$$

$$E_{38} = \int_s (A_{16}y - B_{16}\cos\theta)(r - \frac{F}{2t})ds \tag{27f}$$

$$E_{45} = \int_s \Big[A_{16}\frac{F}{2t}\omega + B_{16}(\omega - \frac{Fq}{2t}) - D_{16}q\Big]ds \tag{27g}$$

$$E_{48} = \int_s (A_{16}\omega - B_{16}q)(r - \frac{F}{2t})ds \tag{27h}$$

$$E_{55} = \int_s (A_{66}\frac{F^2}{4t^2} + B_{66}\frac{F}{t} + D_{66})ds \tag{27i}$$

$$E_{56} = \int_s (A_{66}\frac{F}{2t} + B_{66})\cos\theta ds \tag{27j}$$

$$E_{57} = \int_s (A_{66}\frac{F}{2t} + B_{66})\sin\theta ds \tag{27k}$$

$$E_{58} = \int_s (A_{66}\frac{F}{2t} + B_{66})(r - \frac{F}{2t})ds \tag{27l}$$

$$E_{68} = \int_s \Big[A_{66}(r - \frac{F}{2t})\cos\theta - A_{55}q\sin\theta\Big]ds \tag{27m}$$

$$E_{78} = \int_s \Big[A_{66}(r - \frac{F}{2t})\sin\theta + A_{55}q\cos\theta\Big]ds \tag{27n}$$

$$E_{88} = \int_s \Big[A_{66}(r - \frac{F}{2t})^2 + A_{55}q^2\Big]ds \tag{27o}$$

where A_{ij}, B_{ij} and D_{ij} matrices are extensional, coupling and bending stiffness, respectively, defined by

$$(A_{ij}, B_{ij}, D_{ij}) = \int \bar{Q}_{ij}(1, n, n^2)dn \tag{28}$$

Other values of E_{ij} can be found in Ref.[14]. The explicit forms of the laminate stiffnesses E_{ij} can be calculated for composite box section are given in the Appendix.

V. GOVERNING EQUATIONS

The equilibrium equations of the present study can be obtained by integrating the derivatives of the varied quantities by parts and collecting the coefficients of $\delta W, \delta U, \delta V, \delta\Phi, \delta\Psi_y, \delta\Psi_x$ and $\delta\Psi_\omega$

$$
\begin{aligned}
N_z' &= 0 && \text{(29a)}\\
V_x' &= 0 && \text{(29b)}\\
V_y' &= \mathcal{V}_y && \text{(29c)}\\
M_t' + T' &= \mathcal{T} && \text{(29d)}\\
M_y' - V_x &= 0 && \text{(29e)}\\
M_x' - V_y &= 0 && \text{(29f)}\\
M_\omega' + M_t - T &= 0 && \text{(29g)}
\end{aligned}
$$

The natural boundary conditions are of the form

$$
\begin{aligned}
\delta W &: N_z && \text{(30a)}\\
\delta U &: V_x && \text{(30b)}\\
\delta V &: V_y && \text{(30c)}\\
\delta\Phi &: T + M_t && \text{(30d)}\\
\delta\Psi_y &: M_y && \text{(30e)}\\
\delta\Psi_x &: M_x && \text{(30f)}\\
\delta\Psi_\omega &: M_\omega && \text{(30g)}
\end{aligned}
$$

The 7^{th} denotes the warping restraint boundary condition. When the warping of the cross section is restrained, $\Psi_\omega = 0$ and when the warping is not restrained, $M_\omega = 0$.

By substituting Eqs.(15), (26) into Eq.(29) the explicit form of the governing equations can be expressed with respect to the laminate stiffnesses E_{ij} as

$$
\begin{aligned}
&E_{11}W'' + E_{16}U'' + E_{17}V'' + (E_{15}+E_{18})\Phi'' + E_{12}\Psi_y'' + E_{16}\Psi_y' + E_{13}\Psi_x''\\
&\quad + E_{17}\Psi_x' + E_{14}\Psi_\omega'' + (E_{18}-E_{15})\Psi_\omega' = 0 && \text{(31a)}\\
&E_{16}W'' + E_{66}U'' + E_{67}V'' + (E_{56}+E_{68})\Phi'' + E_{26}\Psi_y'' + E_{66}\Psi_y' + E_{36}\Psi_x''\\
&\quad + E_{67}\Psi_x' + E_{46}\Psi_\omega'' + (E_{68}-E_{56})\Psi_\omega' = 0 && \text{(31b)}\\
&E_{17}W'' + E_{67}U'' + E_{77}V'' + (E_{57}+E_{78})\Phi'' + E_{27}\Psi_y'' + E_{67}\Psi_y' + E_{37}\Psi_x''\\
&\quad + E_{77}\Psi_x' + E_{47}\Psi_\omega'' + (E_{78}-E_{57})\Psi_\omega' = \mathcal{V}_y && \text{(31c)}\\
&(E_{15}+E_{18})W'' + (E_{56}+E_{68})U'' + (E_{57}+E_{78})V'' + (E_{55}+2E_{58}+E_{88})\Phi''\\
&\quad + (E_{25}+E_{28})\Psi_y'' + (E_{56}+E_{68})\Psi_y' + (E_{35}+E_{38})\Psi_x'' + (E_{57}+E_{78})\Psi_x'\\
&\quad + (E_{45}+E_{48})\Psi_\omega'' + (E_{88}-E_{55})\Psi_\omega' = \mathcal{T} && \text{(31d)}\\
&E_{12}W'' - E_{16}W' + E_{26}U'' - E_{66}U' + E_{27}V'' - E_{67}V' + (E_{25}+E_{28})\Phi''\\
&-(E_{56}+E_{68})\Phi' + E_{22}\Psi_y'' - E_{66}\Psi_y + E_{23}\Psi_x'' + (E_{27}-E_{36})\Psi_x' - E_{67}\Psi_x\\
&\quad + E_{24}\Psi_\omega'' + (E_{28}-E_{25}-E_{46})\Psi_\omega' + (E_{56}-E_{68})\Psi_\omega = 0 && \text{(31e)}\\
&E_{13}W'' - E_{17}W' + E_{36}U'' - E_{67}U' + E_{37}V'' - E_{77}V' + (E_{35}+E_{38})\Phi''\\
&-(E_{57}+E_{78})\Phi' + E_{23}\Psi_y'' + (E_{36}-E_{67})\Psi_y' - E_{67}\Psi_y + E_{33}\Psi_x'' - E_{77}\Psi_x\\
&\quad + E_{34}\Psi_\omega'' + (E_{38}-E_{35}-E_{47})\Psi_\omega' + (E_{57}-E_{78})\Psi_\omega = 0 && \text{(31f)}\\
&E_{14}W'' + (E_{15}-E_{18})W' + E_{46}U'' + (E_{56}-E_{68})U' + E_{47}V'' + (E_{57}-E_{78})V'\\
&\quad + (E_{45}+E_{48})\Phi'' + (E_{55}-E_{88})\Phi' + E_{24}\Psi_y'' + (E_{25}-E_{28}+E_{46})\Psi_y'\\
&\quad + (E_{56}-E_{68})\Psi_y + E_{34}\Psi_x'' + (E_{35}-E_{38}+E_{47})\Psi_x' + (E_{57}-E_{78})\Psi_x\\
&\quad + E_{44}\Psi_\omega'' - (E_{55}-2E_{58}+E_{88})\Psi_\omega = 0 && \text{(31g)}
\end{aligned}
$$

Eq.(31) is most general form of a thin-walled laminated composite with a box section. For general anisotropic materials, the dependent variables, U, V, W, Φ, Ψ_x, Ψ_y and Ψ_ω are fully-coupled implying that the beam undergoes

a coupled behavior involving bending, twising, extension, transverse shearing, and warping. If all the coupling effects are neglected, Eq.(31) can be simplified to the uncoupled differential equations as

$$(EA)_{com}W'' = 0 \tag{32a}$$
$$(GA_y)_{com}(U'' + \Psi_y') = 0 \tag{32b}$$
$$(GA_x)_{com}(V'' + \Psi_x') = \mathcal{V}_y \tag{32c}$$
$$\Big[(GJ_1)_{com} + (GJ_3)_{com}\Big]\Phi'' - (GJ_2)_{com}\Psi_\omega' = \mathcal{T} \tag{32d}$$
$$(EI_y)_{com}\Psi_y'' - (GA_y)_{com}(U' + \Psi_y) = 0 \tag{32e}$$
$$(EI_x)_{com}\Psi_x'' - (GA_x)_{com}(V' + \Psi_x) = 0 \tag{32f}$$
$$(EI_\omega)_{com}\Psi_\omega'' + (GJ_2)_{com}\Phi' - \Big[(GJ_1)_{com} - (GJ_3)_{com}\Big]\Psi_\omega = 0 \tag{32g}$$

From above equations, $(EA)_{com}$ represents axial rigidity; $(GA_x)_{com}$, $(GA_y)_{com}$ represent shear rigidities with respect to x and y axis; $(EI_x)_{com}$ and $(EI_y)_{com}$ represent flexural rigidities with respect to x and y axis; $(EI_\omega)_{com}$ represents warping rigidity; and $(GJ_1)_{com}$, $(GJ_2)_{com}$, $(GJ_3)_{com}$ represent torsional rigidities of the thin-walled composite, respectively, written as

$$(EA)_{com} = E_{11} \tag{33a}$$
$$(EI_y)_{com} = E_{22} \tag{33b}$$
$$(EI_x)_{com} = E_{33} \tag{33c}$$
$$(EI_\omega)_{com} = E_{44} \tag{33d}$$
$$(GA_y)_{com} = E_{66} \tag{33e}$$
$$(GA_x)_{com} = E_{77} \tag{33f}$$
$$(GJ_1)_{com} = E_{55} + E_{88} \tag{33g}$$
$$(GJ_2)_{com} = E_{55} - E_{88} \tag{33h}$$
$$(GJ_3)_{com} = 2E_{58} \tag{33i}$$

For bending analysis with respect to x-axis, only Eqs.(32c) and (32f) are involved, and these equations are well-known as Timoshenko beam equations.

VI. FINITE ELEMENT FORMULATION

The present theory for thin-walled composite beams described in the previous section was implemented via a one-dimensional displacement-based finite element method. The generalized displacements are expressed over each element as a linear combination of the one-dimensional Lagrange interpolation function $\widehat{\phi_j}$ associated with node j and the nodal values

$$W = \sum_{j=1}^{n} w_j\widehat{\phi_j} \tag{34a}$$
$$U = \sum_{j=1}^{n} u_j\widehat{\phi_j} \tag{34b}$$
$$V = \sum_{j=1}^{n} v_j\widehat{\phi_j} \tag{34c}$$
$$\Phi = \sum_{j=1}^{n} \phi_j\widehat{\phi_j} \tag{34d}$$
$$\Psi_y = \sum_{j=1}^{n} \psi_{yj}\widehat{\phi_j} \tag{34e}$$
$$\Psi_x = \sum_{j=1}^{n} \psi_{xj}\widehat{\phi_j} \tag{34f}$$

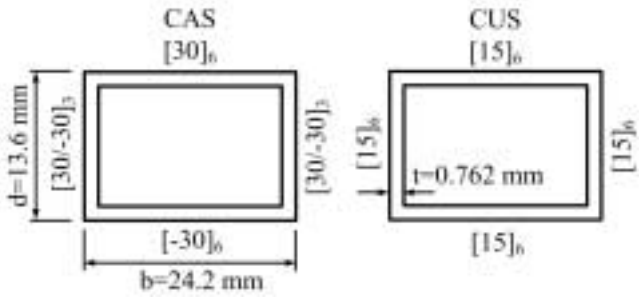

FIG. 2 Geometry and stacking sequence of thin-walled composite beam for verification

$$\Psi_\omega \;=\; \sum_{j=1}^{n} \psi_{\omega j}\widehat{\phi_j} \tag{34g}$$

Substituting these expressions into the weak statement in Eq.(23), the finite element model of a typical element can be expressed as

$$\begin{bmatrix} K_{11} & K_{12} & K_{13} & K_{14} & K_{15} & K_{16} & K_{17} \\ & K_{22} & K_{23} & K_{24} & K_{25} & K_{26} & K_{27} \\ & & K_{33} & K_{34} & K_{35} & K_{36} & K_{37} \\ & & & K_{44} & K_{45} & K_{46} & K_{47} \\ & & & & K_{55} & K_{56} & K_{57} \\ & & & & & K_{66} & K_{67} \\ \text{sym.} & & & & & & K_{77} \end{bmatrix} \begin{Bmatrix} w \\ u \\ v \\ \phi \\ \psi_y \\ \psi_x \\ \psi_\omega \end{Bmatrix} = \begin{Bmatrix} 0 \\ 0 \\ f_3 \\ f_4 \\ 0 \\ 0 \\ 0 \end{Bmatrix} \tag{35a}$$

where $[K]$ is the element stiffness matrix and $[f]$ is the element force vector. More detailed explanation explicit forms of $[K]$ and $[f]$ can be found in Ref.[14].

VII. NUMERICAL EXAMPLES

For verification purpose, a cantilever composite box beam with length $l = 0.762m$, the cross section and the stacking sequences shown in Fig.2 is subjected to a $4.45N$ tip shear load. For all the analyses, the assumption ($\sigma_s = 0$) is made. The following material properties are used

$$E_1 = 141.96\text{GPa}\,, E_2 = 9.79\text{GPa}\,, G_{12} = G_{13} = 6.0\text{GPa}\,, \nu_{12} = 0.34 \tag{36}$$

Ten linear elements with two nodes are used for verification. The resulting of bending slope and the angle of twist using present analysis are compared with previous available results for two stacking sequences CAS, CUS in Figs.3,4 and 5. It is seen that the results by the present analysis are in good agreement with the solution in Ref.[4,6,8].

In order to investigate the coupling, the transverse shear deformation and warping restraint effects, a clamped composite box beam under an eccentric uniform load $\mathcal{V}_y$=-6.5 KN/m is considered (Fig.6). The loads with respect to shear center are $\mathcal{V}_y$=-6.5 KN/m and $\mathcal{T}$=-0.325 KNm/m. For convenience, the following nondimensional values of angle of twist, vertical displacement and shear deformation parameter are used

$$\bar{\phi} \;=\; \frac{\phi E_2 b_1^3}{\mathcal{V}_y l^3} \tag{37a}$$

$$\bar{v} \;=\; \frac{v E_2 b_1^3}{\mathcal{V}_y l^4} \tag{37b}$$

$$\alpha \;=\; \frac{v_s}{v} \tag{37c}$$

where v_s are the vertical displacement due to the shear deformation.

In Fig.7, shear deformation parameter α with respect to the span-to-height ratio for different symmetric and unsymmetric lay-ups are compared with Ref[9]. It is seen that all the results are in excellent agreement.

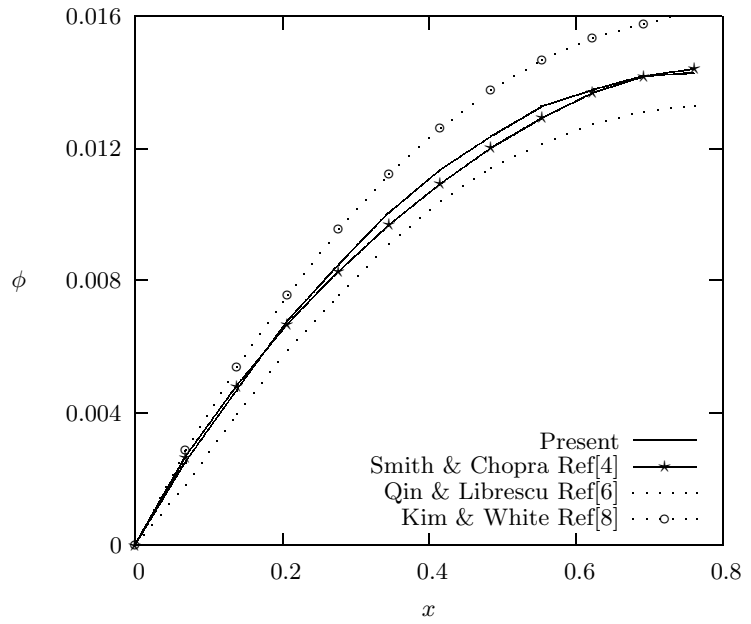

FIG. 3 Angle of twist distribution along a cantilever beam with the CAS lay-up and subjected to a 4.45 N load at its tip

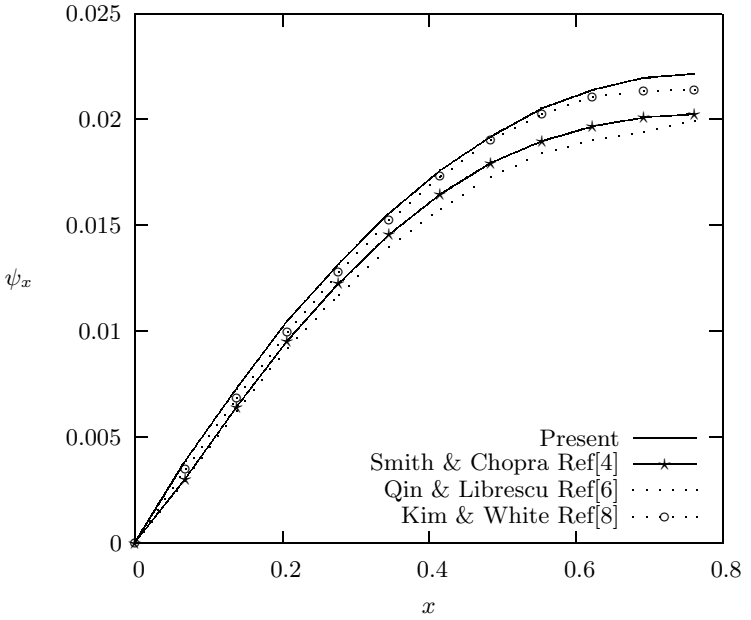

FIG. 4 Bending slope distribution along a cantilever beam with the CAS lay-up and subjected to a 4.45 N load at its tip

Two layers with equal thickness are considered as an anti-symmetric angle-ply laminate $[\theta/-\theta]$ in the flanges and webs (Fig.8a). By using warping restraint (WR) and free warping (FW) model, the maximum angle of twist and the vertical displacement at mid-span of the beam with respect to the fiber angle change are shown in Figs.9 and 10 for $l/b_1 = 10$ and $l/b_1 = 50$. In generating Figs.9 and 10, the finite element solution with no shear effects is calculated based on previous research [13]. The angle of twist is not affected by shear deformation as shown in Fig.9 even for lower span-to-height ratio ($l/b_1 = 10$). That is, the shear deformation due to torsion is negligibly small for flexural-torsional behavior of closed-section. Besides, Figs.9 and 10 also show the influence of warping restraint effects on the angle of twist and the vertical displacement. It is observed that in the investigated case, the warping restraint has a stiffening effect. Thus, the significant discrepancy between warping restraint (WR) and free warping (FW) models

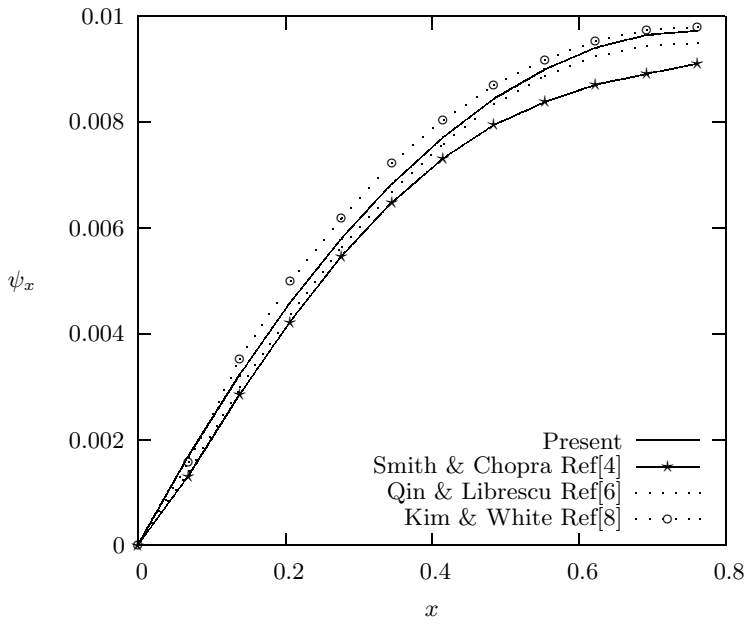

FIG. 5 Bending slope distribution along a cantilever beam with the CUS lay-up and subjected to a 4.45 N load at its tip

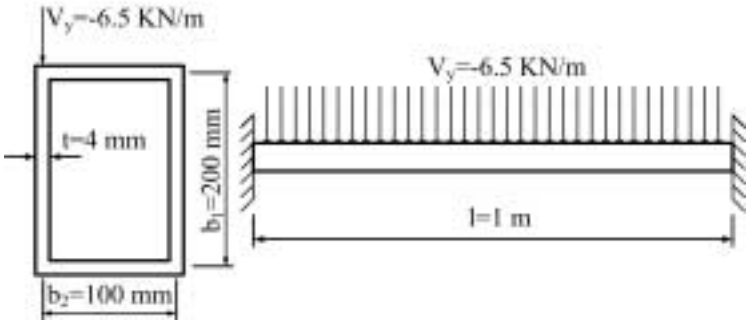

FIG. 6 A clamped composite box beam under an eccentric uniform load

occurs only on the the twist deformation, especially for unidirectional fiber angle, while for the vertical displacement, the influence of warping becomes immaterial. The orthotropy solution of the maximum vertical displacement for the uncoupled equations as given in Eq.(32) can be directly calculated for the beam with uniformly-distributed loading and clamped boundary conditions as

$$v_{max} = \frac{\mathcal{V}_y l^4}{384(EI_x)_{com}} + \frac{\mathcal{V}_y l^2}{8(GA_x)_{com}} \tag{38}$$

In Eq.(38), the first term denotes the displacement by the classical beam theory, and the second term is the displacement by the shear deformation. For this stacking sequence, the coupling stiffnesses E_{15}, E_{27}, E_{36} and E_{48} do not vanish while all the other coupling stiffnesses become zero. That is, the orthotropy solution given in Eq.(38) might not be accurate. However, since the coupling stiffnesses are very small compared to the bending stiffness E_{33} (Table I), the coupling effects coming from the material anisotropy become negligible. Consequently, the finite element solution with warping restraint (WR), free warping (FW) model and the simple orthotropy solution of the classical beam theory agree well as shown in Fig.10.

To investigate the coupling and transverse shear effects further, the same configuration with the previous example except the laminate stacking sequence is considered. Stacking sequence of the top flange and the left web are $[\theta/-\theta]_s$, while the bottom flange and the right web are assumed unidirectional (Fig.8b). For this stacking sequence, the coupling stiffnesses $E_{23}, E_{24}, E_{25}, E_{34}, E_{35}, E_{45}, E_{56}, E_{57}, E_{58}, E_{68}$ and E_{78} do not vanish while all the other coupling stiffnesses become zero. Especially, $E_{23}, E_{56}, E_{57}, E_{68}$ and E_{78} become no more negligibly small as given in Table

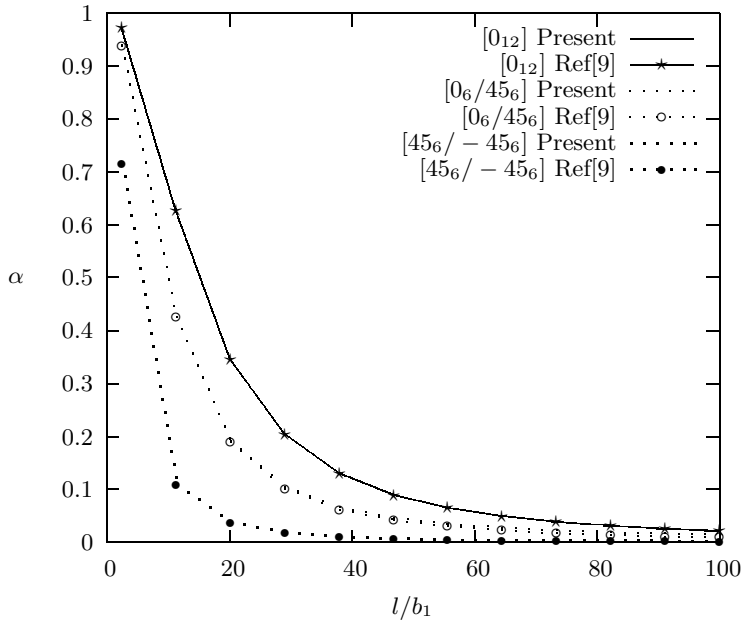

FIG. 7 Shear deformation parameter ($\alpha = v_s/v$) with respect to span-to-height change on a clamped composite box beam under an eccentric uniform load with orthotropic layup

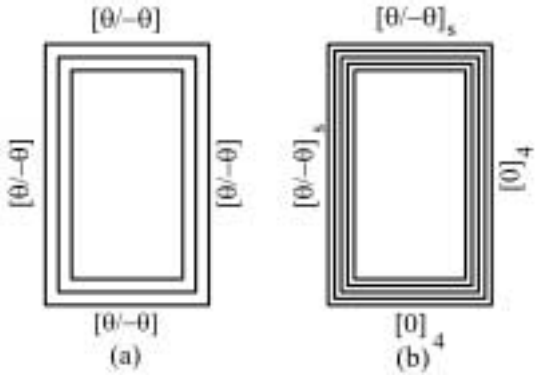

FIG. 8 Geometry and stacking sequence of thin-walled composite beam

TABLE I Ratio of coupling stiffnesses with respect to the bending stiffness and shear deformation parameter α when flanges and webs are all antisymmetric angle-ply

Fiber angle	E_{15}/E_{33}	E_{27}/E_{33}	E_{36}/E_{33}	E_{48}/E_{33}	Shear deformation parameter α	
					Ratio $l/b_1 = 10$	Ratio $l/b_1 = 50$
0	0.000	0.000	0.000	0.000	0.684	0.080
15	-0.044	-0.029	0.015	0.000	0.528	0.043
30	-0.083	-0.055	0.028	0.000	0.266	0.014
45	-0.076	-0.051	0.025	0.000	0.136	0.006
60	-0.024	-0.016	0.008	0.000	0.112	0.005
75	-0.001	-0.001	0.000	0.000	0.119	0.005
90	0.000	0.000	0.000	0.000	0.124	0.006

TABLE II Ratio of coupling stiffnesses with respect to the bending stiffness and shear deformation parameter α when the bottom flange and the right web are unidirectional while the top flange and the left web are symmetric angle-ply

Fiber angle	E_{23}/E_{33}	E_{56}/E_{33}	E_{57}/E_{33}	E_{68}/E_{33}	E_{78}/E_{33}	Shear deformation parameter α	
						Ratio $l/b_1 = 10$	Ratio $l/b_1 = 50$
0	0.000	0.000	0.000	0.000	0.000	0.684	0.080
15	0.002	-0.057	-0.115	-0.129	-0.085	0.644	0.070
30	0.055	-0.136	-0.273	-0.393	-0.377	0.597	0.058
45	0.147	-0.099	-0.199	-0.380	-0.462	0.506	0.045
60	0.178	-0.041	-0.082	-0.235	-0.347	0.445	0.037
75	0.182	-0.009	-0.019	-0.147	-0.265	0.415	0.032
90	0.182	0.000	0.000	-0.120	-0.239	0.406	0.027

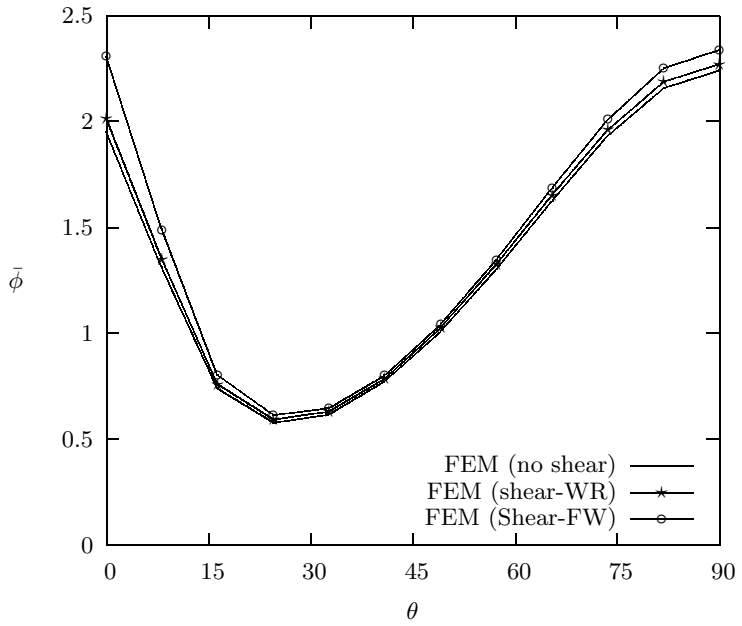

FIG. 9 Variation of angle of twist at mid-span with respect to fiber angle change in the flanges and webs for a clamped composite box beams under an eccentric uniform load with ratio $l/b_1 = 10$

II. Shear deformation parameter α in Table II shows that the shear effects are significant even for higher fiber angle for $l/b_1 = 10$. For lower span-to-height ratio (Fig.11), however, the solutions excluding shear effects remarkably underestimate the displacement for all the range of fiber angle. The orthotropy solutions disagree with the finite element solutions as anisotropy of the beam gets higher and fiber angle increases. For $l/b_1 = 50$, as fiber angle increases, the orthotropy solution and the finite element solution show discrepancy indicating the coupling effects become significant (Fig.12). The shear effects are negligible in this case.

VIII. CONCLUDING REMARKS

An analytical model was developed to study the flexural behavior of a laminated composite beam with box section. The model is capable of predicting accurate deflection for various configuration including boundary conditions, laminate orientation and span-to-height ratio. To formulate the problem, a one-dimensional displacement-based finite element method is employed. The shear effects become significant for lower span-to-height ratio and higher degrees of orthotropy of the beam. The orthotropy solution is accurate for lower degrees of material anisotropy, but, becomes inappropriate as the anisotropy of the beam gets higher, and fully coupled equations should be considered for accurate analysis of thin-walled composite beams. The presented analytical model is found to be appropriate and efficient in analyzing flexural problem of thin-walled laminated composite box beams.

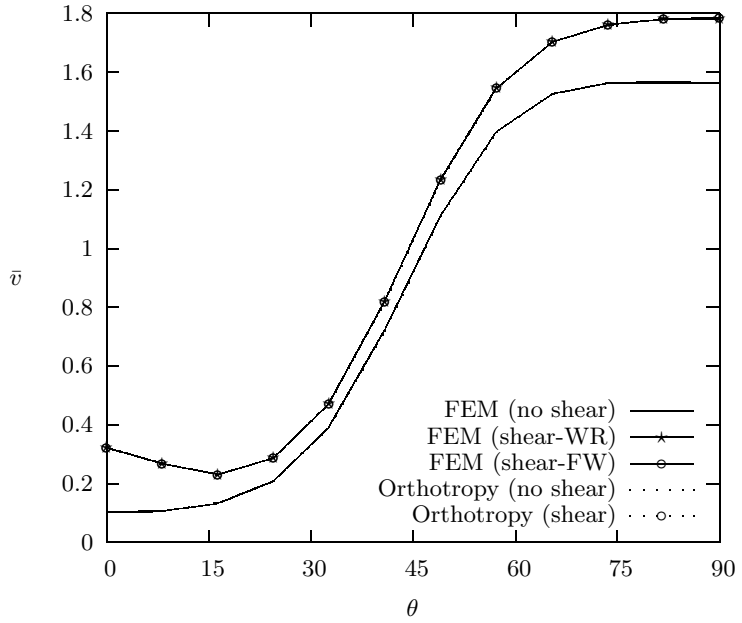

FIG. 10 Variation of the vertical displacements at mid-span with respect to fiber angle change in the flanges and webs for a clamped composite box beams under an eccentric uniform load with ratio $l/b_1 = 10$

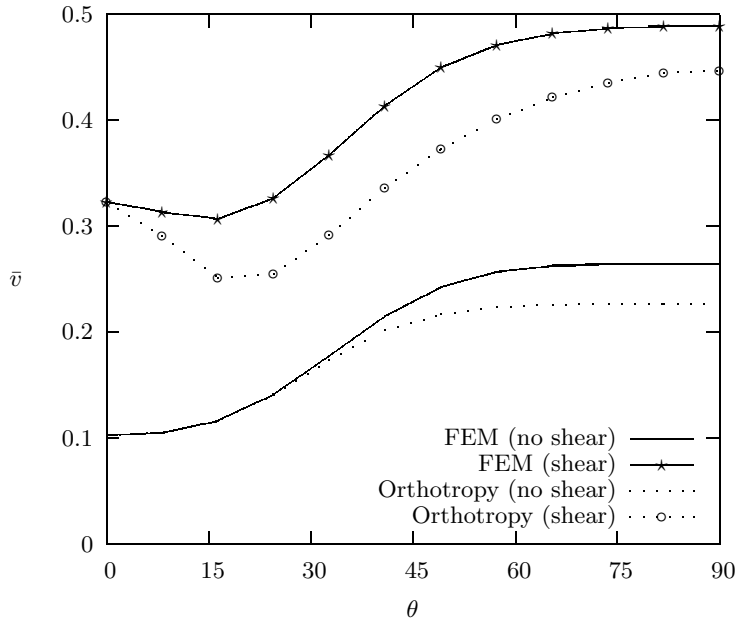

FIG. 11 Variation of the vertical displacements at mid-span with respect to fiber angle change in the top flange and the left web for a clamped composite box beams under an eccentric uniform load with ratio $l/b_1 = 10$

Acknowledgments

The support of the research reported here by Korea Ministry of Construction and Transportation through Grant 2002-F02-01 is gratefully acknowledged.

APPENDIX

The explicit forms of the laminate stiffnesses E_{ij} for composite box section in Fig.13 can be defined by

$$E_{16} = A_{16}^2 b_2 - A_{16}^4 b_2 \tag{39a}$$

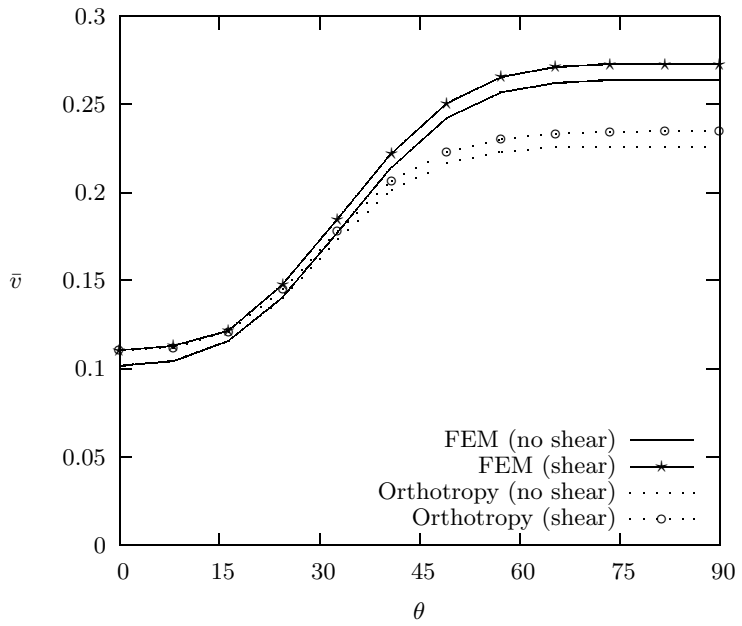

FIG. 12 Variation of the vertical displacements at mid-span with respect to fiber angle change in the top flange and the left web for a clamped composite box beams under an eccentric uniform load with ratio $l/b_1 = 50$

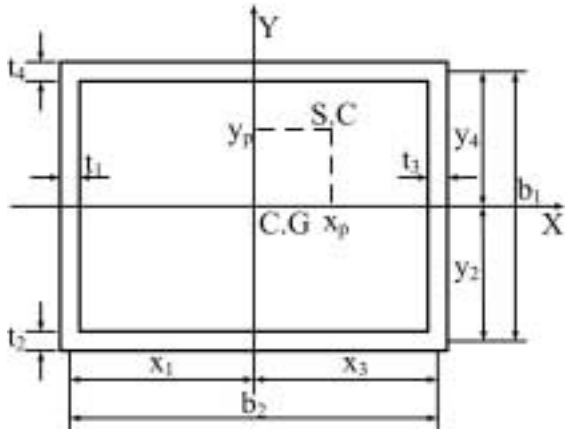

FIG. 13 Geometry of thin-walled composite box section

$$E_{17} = -A^1_{16}b_1 + A^3_{16}b_1 \tag{39b}$$

$$E_{18} = A^1_{16}(-x_1 + x_p - \frac{F}{2t_1})b_1 + A^2_{16}(-y_2 + y_p - \frac{F}{2t_2})b_2 + A^3_{16}(x_3 - x_p - \frac{F}{2t_3})b_1 + A^4_{16}(y_4 - y_p - \frac{F}{2t_4})b_2 \tag{39c}$$

$$E_{26} = \frac{1}{2}A^2_{16}b_2^2 + A^2_{16}x_1b_2 + \frac{1}{2}A^4_{16}b_2^2 - A^4_{16}x_3b_2 \tag{39d}$$

$$E_{27} = -A^1_{16}x_1b_1 + B^1_{16}b_1 + A^3_{16}x_3b_1 + B^3_{16}b_1 \tag{39e}$$

$$\begin{aligned} E_{28} &= (A^1_{16}x_1 - B^1_{16})(-x_1 + x_p - \frac{F}{2t_1})b_1 + \frac{1}{2}A^2_{16}(-y_2 + y_p - \frac{F}{2t_2})b_2^2 + A^2_{16} * x_1(-y_2 + y_p - \frac{F}{2t_2})b_2 \\ &+ (A^3_{16}x_3 + B^3_{16})(x_3 - x_p - \frac{F}{2t_3})b_1 - \frac{1}{2}A^4_{16}(y_4 - y_p - \frac{F}{2t_4})b_2^2 + A^4_{16}x_3(y_4 - y_p - \frac{F}{2t_4})b_2 \end{aligned} \tag{39f}$$

$$E_{36} = A^2_{16}y_2b_2 - B^2_{16}b_2 - A^4_{16}y_4b_2 - B^4_{16}b_2 \tag{39g}$$

$$E_{37} = \frac{1}{2}A^1_{16}b_1^2 - A^1_{16}y_4b_1 + \frac{1}{2}A^3_{16}b_1^2 + A^3_{16}y_2b_1 \tag{39h}$$

$$E_{38} = -\frac{1}{2}A^1_{16}(-x_1+x_p-\frac{F}{2t_1})b_1^2 + A^1_{16}y_4(-x_1+x_p-\frac{F}{2t_1})b_1 + (A^2_{16}y_2 - B^2_{16})(-y_2+y_p-\frac{F}{2t_2})b_2$$
$$+ \frac{1}{2}A^3_{16}(x_3-x_p-\frac{F}{2t_3})b_1^2 + A^3_{16}y_2(x_3-x_p-\frac{F}{2t_3})b_1 + (A^4_{16}y_4 + B^4_{16})(y_4-y_p-\frac{F}{2t_4})b_2 \quad (39i)$$

$$E_{46} = \frac{1}{2}(A^2_{16}A_2 - B^2_{16})b_2^2 + A^2_{16}(A_1b_1+C)b_2$$
$$+ \frac{1}{2}(-A^4_{16}A_4 + B^4_{16})b_2^2 - A^4_{16}(C+A_1b_1+A_2b_2+A_3b_1)b_2 \quad (39j)$$

$$E_{47} = \frac{1}{2}(-A^1_{16}A_1 + B^1_{16})b_1^2 - A^1_{16}Cb_1 + \frac{1}{2}(A^3_{16}A_3 - B^3_{16})b_1^2 + A^3_{16}(A_1b_1+A_2b_2+C)b_1 \quad (39k)$$

$$E_{48} = \frac{1}{2}(A^1_{16}A_1 - B^1_{16})(-x_1+x_p-\frac{F}{2t_1})b_1^2 + A^1_{16}C(-x_1+x_p-\frac{F}{2t_1})b_1$$
$$+ \frac{1}{2}(A^2_{16}A_2 - B^2_{16})(-y_2+y_p-\frac{F}{2t_2})b_2^2 + A^2_{16}(A_1b_1+C)(-y_2+y_p-\frac{F}{2t_2})b_2$$
$$+ \frac{1}{2}(A^3_{16}A_3 - B^3_{16})(x_3-x_p-\frac{F}{2t_3})b_1^2 + A^3_{16}(A_1b_1+A_2b_2+C)(x_3-x_p-\frac{F}{2t_3})b_1$$
$$+ \frac{1}{2}(A^4_{16}A_4 - B^4_{16})(y_4-y_p-\frac{F}{2t_4})b_2^2 + A^4_{16}(C+A_1b_1+A_2b_2+A_3b_1)(y_4-y_p-\frac{F}{2t_4})b_2 \quad (39l)$$

$$E_{56} = A^2_{66}\frac{F}{2t_2}b_2 + B^2_{66}b_2 - A^4_{66}\frac{F}{2t_4}b_2 - B^4_{66}b_2 \quad (39m)$$

$$E_{57} = -A^1_{66}\frac{F}{2t_1}b_1 - B^1_{66}b_1 + A^3_{66}\frac{F}{2t_3}b_1 + B^3_{66}b_1 \quad (39n)$$

$$E_{58} = (A^1_{66}\frac{F}{2t_1} + B^1_{66})(-x_1+x_p-\frac{F}{2t_1})b_1 + (A^2_{66}\frac{F}{2t_2} + B^2_{66})(-y_2+y_p-\frac{F}{2t_2})b_2$$
$$+ (A^3_{66}\frac{F}{2t_3} + B^3_{66})(x_3-x_p-\frac{F}{2t_3})b_1 + (A^4_{66}\frac{F}{2t_4} + B^4_{66})(y_4-y_p-\frac{F}{2t_4})b_2 \quad (39o)$$

$$E_{66} = A^1_{55}b_1 + A^2_{66}b_2 + A^3_{55}b_1 + A^4_{66}b_2 \quad (39p)$$

$$E_{67} = 0 \quad (39q)$$

$$E_{68} = -\frac{1}{2}A^1_{55}b_1^2 + A^2_{66}(-y_2+y_p-\frac{F}{2t_2})b_2 + \frac{1}{2}A^3_{55}b_1^2 - A^4_{66}(y_4-y_p-\frac{F}{2t_4})b_2 \quad (39r)$$

$$E_{77} = A^1_{66}b_1 + A^2_{55}b_2 + A^3_{66}b_1 + A^4_{55}b_2 \quad (39s)$$

$$E_{78} = -A^1_{66}(-x_1+x_p-\frac{F}{2t_1})b_1 + A^3_{66}(x_3-x_p-\frac{F}{2t_3})b_1 \quad (39t)$$

$$E_{88} = A^1_{66}(-x_1+x_p-\frac{F}{2t_1})^2b_1 + \frac{1}{3}A^1_{55}b_1^3 + A^2_{66}(-y_2+y_p-\frac{F}{2t_2})^2b_2 + \frac{1}{3}A^2_{55}b_2^3$$
$$+ A^3_{66}(x_3-x_p-\frac{F}{2t_3})^2b_1 + \frac{1}{3}A^3_{55}b_1^3 + A^4_{66}(y_4-y_p-\frac{F}{2t_4})^2b_2 + \frac{1}{3}A^4_{55}b_2^3 \quad (39u)$$

where the St. Venant circuit shear flow F, the warping functions with respect to the shear center of side 1, 2, 3, 4 $\omega_1(s_1), \omega_1(s_2), \omega_1(s_3), \omega_1(s_4)$ and other values of E_{ij} can be found in Ref.[13]

References

[1] Vlasov, V. Z., *Thin-walled elastic beams*, 2nd Edition, Israel Program for Scientific Translation, Jerusalem, Israel, 1961.

[2] Gjelsvik, A., *The theory of thin-walled bars*, John Wiley and Sons Inc., New York, 1981.

[3] Chandra, R., Stemple, A.D. and Chopra, I. "Thin-walled composite beams under bending, torsional and extensional loads," *J Aircraft*, Vol.27, No. 7, 1990, pp.619-636.

[4] Smith E.C. and Chopra, I. "Formulation and evaluation of an analytical model for composite box-beams," *J Am Helicopter Soc*, Vol.36, No.3, 1991, pp.23-35.

[5] Song, 0. and Librescu, L. "Free Vibration Of Anisotropic Composite Thin-Walled Beams Of Closed Cross-Section Contour," *Journal of Sound and Vibration*, Vol.167, No. 1, 1993, pp.129-147.

[6] Qin, Z. and Librescu, L. "On a shear-deformable theory of anisotropic thin-walled beams: further contribution and validations, " *Composite Structures*, Vol.56, No.4, 2002, pp.345-358.

[7] Kim, C. and White, S. R.,"Analysis of thick hollow composite beams under general loadings," *Computer and Structures* Vol.34, 1996, pp.263-277.

[8] Kim, C. and White, S. R.,"Thick-walled composite beam theory including 3-d elastic effects and torsional warping," *Int. J. Solids Structures* Vol. 34, 1997, Nos 31-32, pp. 4237-4259

[9] Pluzsik, A., Kollar, L.P., "Effects of Shear Deformation and Restrained Warping on the Displacements of Composite Beams," *Journal of Reinforced Plastics and Composites*, Vol.21, No. 17, 2002, pp.1423-1465.

[10] Salim, H.A. and Davalos, J.F., "Torsion of Open and Closed Thin-Walled Laminated Composite Sections," *Journal of Composite Materials*, Vol.39, No. 6, 2005, pp.497-524.

[11] Librescu, L. and Song, 0., *Thin-walled Composite Beams*, Springer, 2006.

[12] Piovan, M.T. and Cortinez, V.H. , "Mechanics of shear deformable thin-walled beams made of composite materials," *Thin-Walled Structures*, Vol.45, Issue 1, January 2007, pp. 37-62

[13] Vo, T.P. and Lee, J., "Flexural-torsional behavior of thin-walled closed-section composite box beams," *Engineering Structures*, In Press, Vol.29, 2007

[14] Lee, J., "Flexural analysis of thin-walled composite beams using shear-deformable beam theory," *Composite Structures*, Vol.70, 2005, pp. 212-222.

[15] Timoshenko, S. P. and Gere, J. M., *Theory of Elastic Stability*, McGraw-Hill, New York, 1963.

[16] Jones, R. M., *Mechanics of composite materials*, Hemisphere Publishing Corp., New York, 1975.